

INFLUENCE OF THERMAL ANNEALING IN AIR ON THE STRUCTURAL AND OPTICAL PROPERTIES OF AMORPHOUS ANTIMONY TRISULFIDE THIN FILMS

N. Tigau^{*}, V. Ciupina^a, G. Prodan^a, G. I. Rusu^b, C. Gheorghies, E. Vasile^c

Faculty of Science, "Dunarea de Jos" University, Galati, R-6200, Romania

^a"Ovidius" University, Constanta, R-8700, Romania

^bFaculty of Physics, "Alexandru Ioan Cuza" University, Iasi, R-6600, Romania

^cS.C. METAV S.A, Bucuresti, R-7200, Romania

Amorphous antimony trisulfide films were deposited on glass using thermal vacuum evaporation technique at substrate temperatures $T_S = 300$ K. The films were annealed in air at a temperature of 500 K for 30 minutes. The structure and chemical composition of films were determined by X-ray and electron microscopy investigations. The films are composed of an amorphous structure that includes nanocrystallites of antimony trioxide. The amorphous as-deposited films transform into polycrystalline films during treatment above 500 K. Absorption coefficients of the films were determined using spectrophotometric measurements of the transmittance, T , at normal incidence in the spectral range 460-1400 nm. The optical properties of amorphous film differ substantially from those of polycrystalline films, after heat treatment the direct energy band gap decreases from 2.46 eV to 2.40 eV and the indirect band gap from 1.64 eV to 1.20 eV, respectively.

(Received May 23, 2003; accepted after revision January 29, 2004)

Keywords: Antimony trisulfide, Transmission electron microscopy, Optical properties

1. Introduction

Antimony trisulfide, Sb_2S_3 , has been the subject of intense work because of its diverse applications in the target materials for television cameras [1], microwave devices [2], switching devices [3] and various optoelectronic devices [4-6].

Various methods such as vacuum evaporation; sintering and precipitate, electrodeposition and chemical methods have been employed to prepare Sb_2S_3 thin and thick films [7-13]. From the methods used for the preparation of antimony trisulfide thin films, the thermal vacuum evaporation is often preferred because it offers large possibilities to modify the deposition condition and so to obtain films with determined structure and physical properties.

Post deposition annealing in air changes the optical and electrical properties of the deposition thin films due to the changes in their structure [14].

The objective of this paper was to study the effect of annealing in air at a temperature above crystallization on the structural and optical properties of amorphous antimony trisulfide thin films.

2. Experimental

Thin films of Sb_2S_3 were prepared by thermal vacuum evaporation at about 5×10^{-5} torr, from ingot powder of 99,99 % purity on glass substrates [15]. For investigating the thermal annealing, we have chosen the thin film deposited at substrate temperatures $T_S = 300$ K. The thickness of the

*Corresponding author: ntigau@ugal.ro

antimony trisulfide film ($d = 400$ nm) was determined by an interferometric method (multiple-beam Fizeau fringe method [16]), using an MII-4 type microscope. The post-deposition heat treatment was carried out in air for 30 minutes at temperatures $T_A = 500$ K.

The structure of the thin films, before and after the heat treatment, was examined by X-ray diffraction technique using a Dron 3 diffractometer with $\text{CuK}\alpha$ radiation ($\lambda=1.5418$ Å) and electron microscopy investigations. A transmission electron microscope (Philips CM 120), operating at 100 kV with a calibrated resolution 4 Å, was used for the microstructure study

The optical data were derived from the optical transmission spectra measured by double-beam spectrophotometer (Specord UV-VIS M-40). The films were measured in the spectral range from 400 to 1400 nm at room temperature.

3. Results and discussion

The X-ray diffraction measurements (XRD), obtained for 2θ scans between 20° and 60° , has been made on Sb_2S_3 thin films deposited onto glass at substrate temperatures $T_S=300$ K, in order to obtain their structure. The X-ray diffractogram obtained for Sb_2S_3 composition in a powder form is represented in Fig. 1.

Careful analysis of X-ray diffraction pattern indicates the polycrystalline nature of the orthorhombic structure phase with lattice parameter $a=1.127$ nm, $b=1.129$ nm and $c=0.384$ nm. These values are in agreement with that reported by Salem et al [8] and by Desai et al [9].

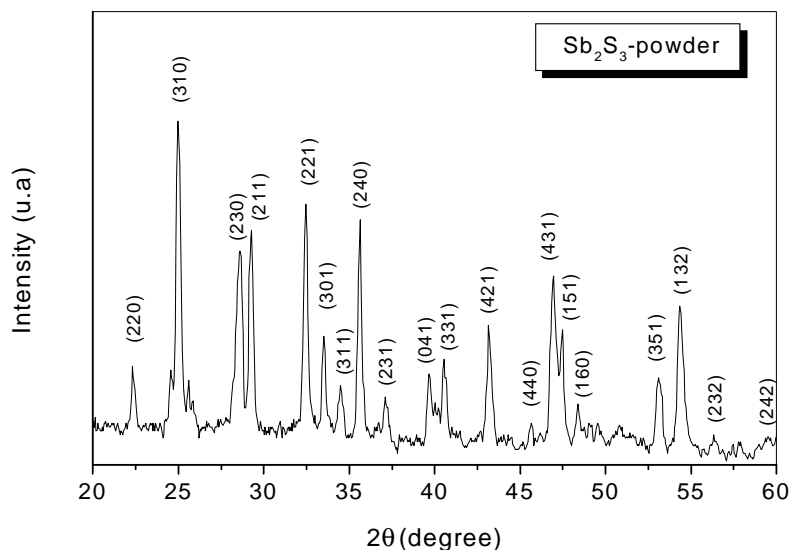


Fig. 1. X-ray diffraction pattern of Sb_2S_3 in a powder form.

Fig. 2 illustrates that the typical X-ray diffractograms of the as-deposited Sb_2S_3 thin films of thickness 400 nm are amorphous (curve a), while those annealed in air for 30 minutes at $T_A = 500$ K become polycrystalline (curve b). This last fact is proved by the appearance of diffraction peaks at 2θ of about 28° , 32° , 55° and 59° , which correspond to diffraction from (211), (221), (132) and (242) planes of Sb_2S_3 orthorhombic unit cell ($a=1.127$ nm, $b=1.129$ nm and $c=0.384$ nm). Other small peaks that appeared in the diffraction patterns of the annealed films (Fig. 2, curve b) indicate a partial oxidation of the samples, as it was to be expected. Thus, after the thermal treatment, the samples contain a mixture of Sb_2S_3 and Sb_2O_3 . We notice in Fig. 2 (b) a small peak at $2\theta=35^\circ$ corresponding to diffraction on the (331) planes of the cubic crystalline structure of Sb_2O_3 . Also in Fig. 2b there are peaks at $2\theta=46^\circ$ that also belong to the antimony oxide, which correspond to diffraction from the (440) planes of cubic unit cell of Sb_2O_3 . The computed lattice parameter of cubic unit cell of Sb_2O_3 is

$a=11.16 \text{ \AA}$ [17]. It appears that the preferred orientation of such grown polycrystalline films is (211), which is parallel to the substrate plane. The interplanar spacing values (d_{hkl}) were calculated and are given in Table 1.

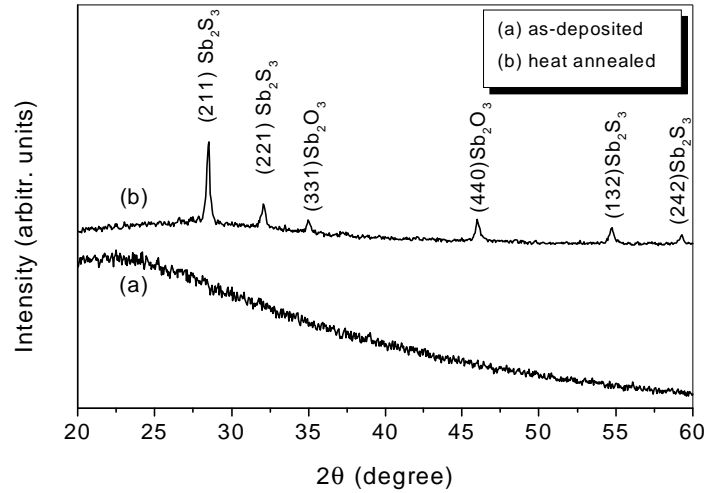


Fig. 2. X-ray diffraction pattern of Sb_2S_3 thin film before and after heat treatment.

Table 1. The interplanar spacing values (d_{hkl}) of heat annealed Sb_2S_3 thin film.

hkl	d_{hkl} (nm)	I/I_0
(211) Sb_2S_3	0.323	100
(221) Sb_2S_3	0.277	22
(331) Sb_2O_3	0.255	12
(440) Sb_2O_3	0.197	25
(132) Sb_2S_3	0.166	18
(242) Sb_2S_3	0.154	11

The same results were obtained by electron diffraction studies of Sb_2S_3 films to check the polycrystalline nature of films after heat treatment. Fig. 3(a) and (3b) shows the transmission electron micrographs (TEM) and the corresponding selected area electron diffraction patterns for Sb_2S_3 thin films, before and after heat treatment, respectively.

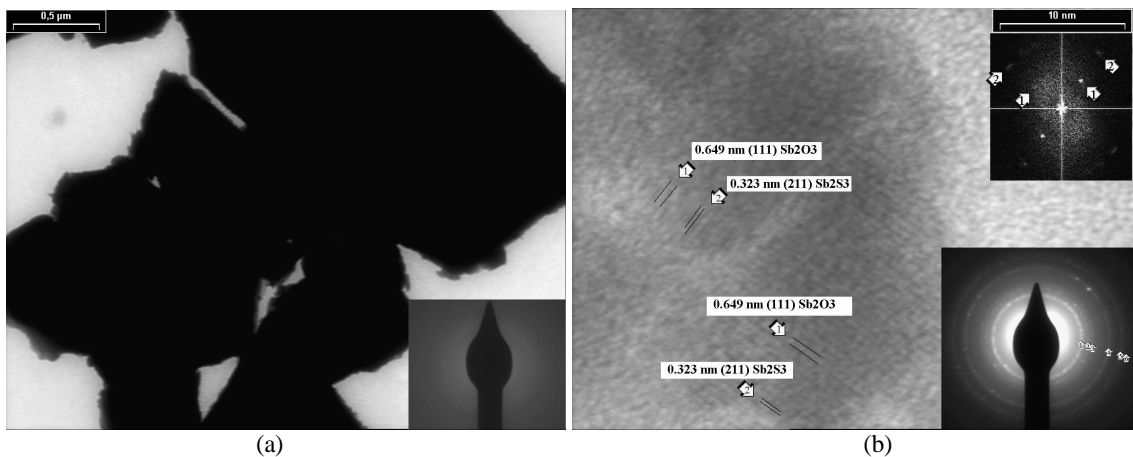


Fig. 3. Transmission electron micrograph of Sb_2S_3 thin films: (a) as-deposited (b) annealed.

The scanning electron micrographs (SEM) showed amorphous featureless structure for as-deposited films at $T_S = 300$ K as seen in Fig. 4(a). The as-deposition films are composed of an amorphous structure that includes nanocrystallites of antimony trioxide. The polycrystalline structure is clear in the micrograph of annealed films at $T_A = 500$ K in Fig. 4(b). This micrograph show randomly distributed particles on the film surface. The grain size is determined to be $1.05 \mu\text{m}$.

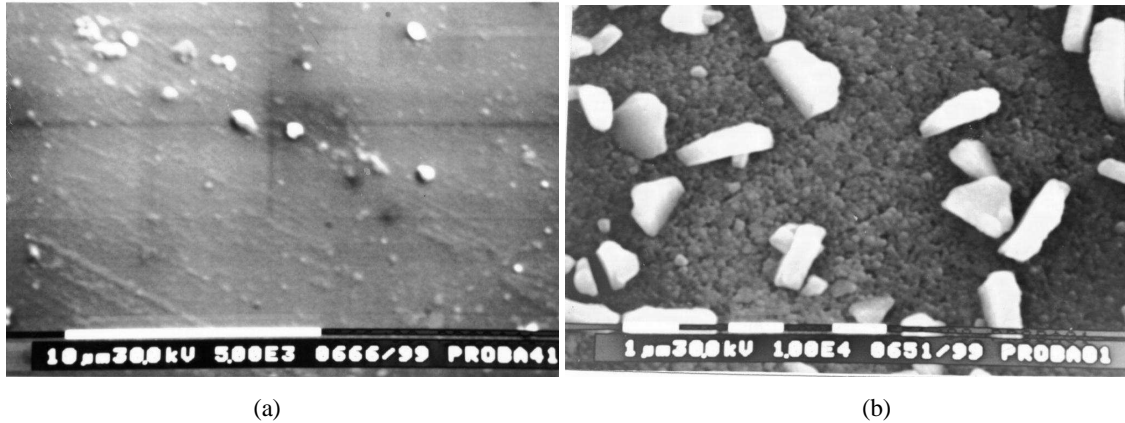


Fig. 4. Scanning electron micrographs of Sb_2S_3 thin films: (a) as-deposited (b) annealed.

The optical properties of the Sb_2S_3 thin films are also influenced by the thermal treatment. In Fig. 5 the transmission spectra in the wavelength range 460-1400 nm for thin films deposited at substrate temperature $T_S = 300$ K, before and after thermal treatment, are presented. The presence of the maxima and minima of the transmission spectrum for the as-deposited films indicates that the films are thin pellicles with plane-parallel surfaces. As it can be seen, after the thermal treatment, the films transmittance decreases. We consider that the lower transmittance of the heat-annealed films is due primarily to the increased of the crystallite size. Also, the increased roughness of the heat-annealed thin films plays an important part in the drastic decrease of optical transmittance. This is due to the destructive interference of the light transmitted through the high and irregular grains of the samples that form nonlevelled surfaces.

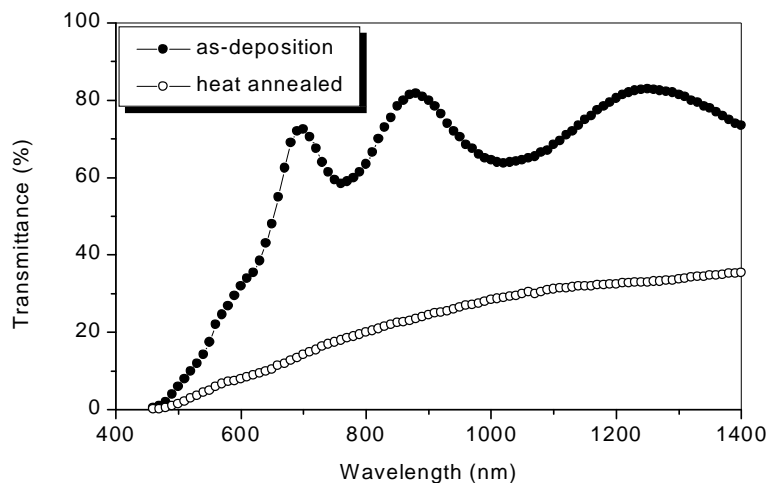


Fig. 5. The dependence of transmittance of Sb_2S_3 thin films on the wavelength.

The dependence of the absorption coefficient, α , of the photon energy is important in studying energy band structure and the type of transition of the electrons. The absorption coefficient, α , was estimated by the transmittance data, using the Swanepoel's method [18] (Fig. 6). In the high photon

energy region, the energy dependence of the absorption coefficient ($\alpha \approx 10^5 \text{ cm}^{-1}$) suggests the occurrence of direct electron transitions. Namely, the great value the absorption coefficient in the range of 2.25 –2.70 eV is due to optical excitations across the direct interband transitions. On the other side, in the range 1-2.25 eV the absorption coefficient indicates indirect interband transitions, and it is smaller compared with the absorption coefficient which is due direct interband transitions.

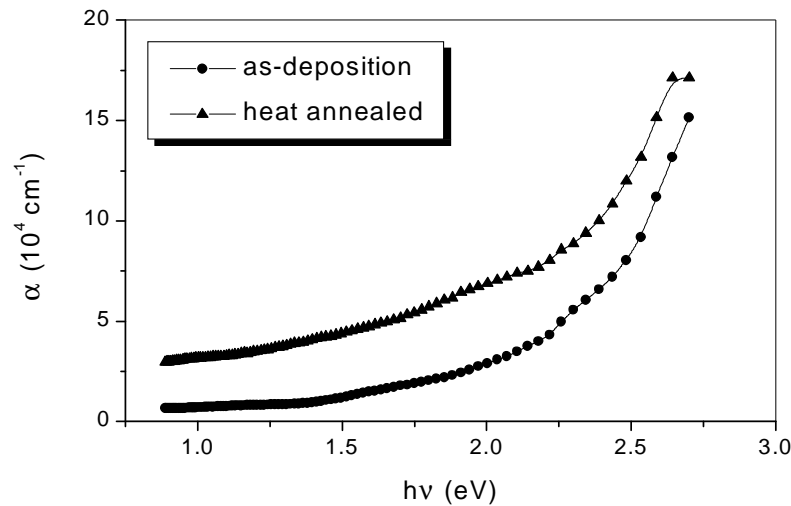


Fig. 6. The dependence of absorption coefficient (α) on photon energy ($h\nu$).

In order to determine the optical band gap of the semiconductor the following dependence of α on the photon energy equation [19] is used:

$$(\alpha h\nu) = B(h\nu - E_g)^n \quad (1)$$

where B is a parameter that depend on the transmission probability, E_g is the band gap energy, α is the absorption coefficient and n is an index that can assume values of (1/2, 2) depending on the nature of the electronic transitions.

For the direct allowed transitions, n has a value of 1/2 and, using a graphic presentation $(\alpha h\nu)^2 = f(h\nu)$ (Fig. 7) on the intercept of the straight part of the curves with the $h\nu$ -axis, the optical band gap of Sb_2S_3 films was estimated. From Fig. 7 we obtain the values for the optical band gap of 2.47 eV and 2.40 eV for as-deposited films and heat annealed film, respectively.

In the theory of indirect interband transitions assisted by phonons, the absorption coefficient can be expressed as [20]:

$$\alpha = \alpha_a + \alpha_e = B_{abs}(h\nu - E_g + E_{ph})^2 + B_{em}(h\nu - E_g - E_{ph})^2 \quad (2)$$

where E_{ph} is the phonon energy and the parameters B_{abs} and B_{em} correspond to the absorption and emission of a phonon, respectively.

The optical band gap of Sb_2S_3 films for indirect transitions was estimated from the intercept of the straight part of the curves with $h\nu$ -axis using a graphic presentation of dependence of $(\alpha h\nu)^{1/2}$ of photon energy (Fig. 8). A great decrease in the indirect optical band gap from 1.64 eV corresponding of as-deposited films to 1.20 eV for annealed films was observed in Fig. 8.

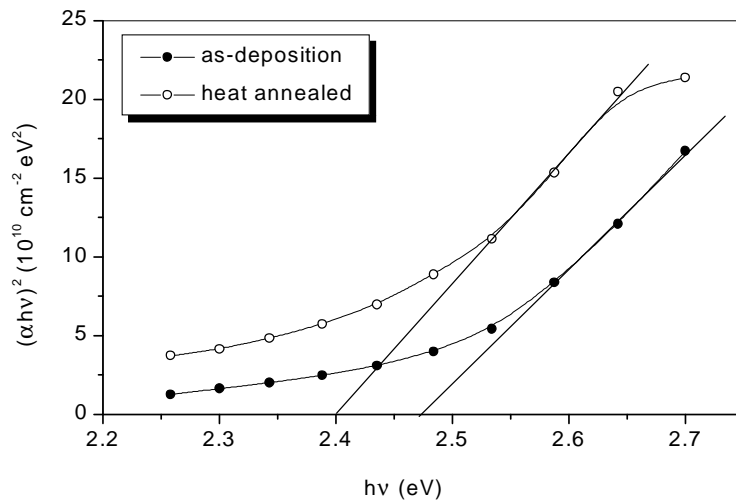


Fig.7. The dependence of $(\alpha h\nu)^2$ on the photon energy ($h\nu$).

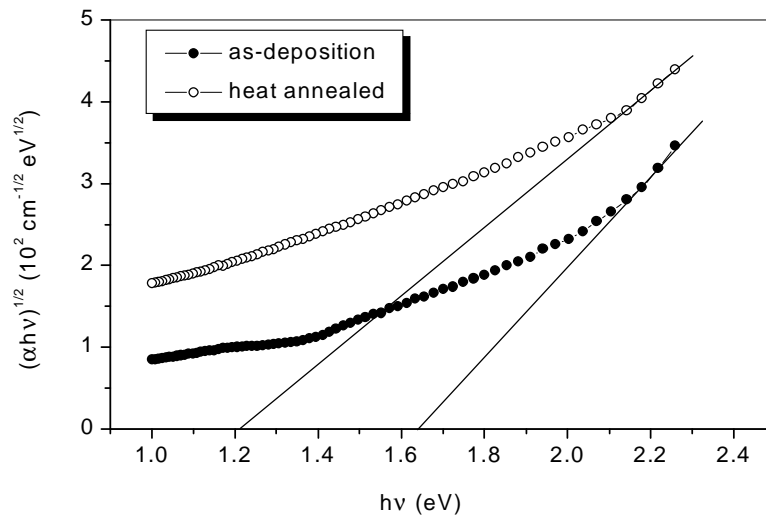


Fig. 8. The dependence of $(\alpha h\nu)^{1/2}$ on the photon energy ($h\nu$).

5. Conclusions

The vacuum evaporation method enabled us to deposit amorphous Sb_2S_3 thin films. Both X-ray and electron microscopy studies indicate a complex structure of the films. The as-deposited films are composed of amorphous matrix that includes nanocrystallites of Sb_2S_3 . The amorphous as-deposited films transform into polycrystalline films during thermal treatment in air at 500 K for 30 minutes.

The calculated optical constants of the Sb_2S_3 thin films indicate that both direct and indirect optical transitions are present. The optical energy band gap due to the direct transitions shows a slightly decreases from 2.46 eV to 2.40 eV after heat treatment. The energy band gap of the existing allowed indirect optical transitions in amorphous Sb_2S_3 films is found to be 1.64 eV and it is decreased to 1.20 eV for polycrystalline films.

References

- [1] G. Ghosh, B. P. Varma, *Thin Solid Films* **69**, 61 (1979).
- [2] J. Grigas, J. Meshkanskas, J. Orlimans, *Physica Status Solidi (A)* **37**, 10 (1976).
- [3] M. S. Ablova, A. A. Andreev, T. T. Degegkaev, B. T. Melekh, A. B. Pevtsov, N. S. Shendel, L. N. Shurnilova *Sov. Phys. Semicond.* **10**, 6 (1976).
- [4] M. J. Chokalingam, K. Nagaraja Rao, R. Rangarajan, C. V. Suryanarayana, *J. Phys. D.: Appl. Phys.* **3**, 1641 (1970).
- [5] E. Montrimass, A. Pazera, *Thin Solid Films* **34**, 65 (1976).
- [6] J. George, M. K. Radhakrishnan, *Solid State Commun.* **33**, 987 (1980).
- [7] I. K. El Zawawi, A. Abdel-Moez, F. S. Terra, M. Mounir, *Thin Solid Films* **324**, 300 (1998).
- [8] A. M. Salem, M. Soliman Selim, *J. Phys.D: Appl. Phys.* **34**, (2001).
- [9] E. Marquez, J. B. Ramirez-Malo, P. Villares, R. Jimenez-Garay, R. J. Swanepoel, *Thin Solid Films* **254**, 83 (1993).
- [10] C. H. Bhosale, M. D. Uplane, P. S. Patil, C. D. Lokhande, *Thin Solid Films* **248**, 137 (1994).
- [11] K. Y. Rajpure, A. L. Dhebe, C. D. Lokhande, C. H. Bhosale, *Materials Chemistry and Physics* **56**, 177 (1998).
- [12] B. R. Sankapal, R. S. Mane, C. D. Lokhande, *Journal of Materials, Science Letters* **18**, 1453 (1999).
- [13] N. S. Yesugade, C. D. Lokhande, C. H. Bhosale, *Thin Solid Films* **263**, 145 (1995).
- [14] I. K. El Zawawi, A. Abdel-Moez, F. S. Terra, M. Mounir, *Fizica* **A7**(3), 97 (1998)
- [15] N. Tigau, G. I. Rusu, C. Gheorghies, *J. Optoelectron. Adv. Mater.* **4**, 943 (2002)
- [16] K. L. Chopra, *Thin Film Phenomena*, McGraw-Hill, New York, 1969
- [17] N. Tigau, V. Ciupina, G. Prodan, G. I. Rusu, C. Gheorghies, E. Vasile, *J. Optoelectron. Adv. Mater.* **4**, 907 (2003)
- [18] R. J. Swanepoel *J. Phys. E. Sci. Instrum.* **16**, 1214 (1983)
- [19] J. Tauc (ed.), *Amorphous and Liquid Semiconductors*, North-Holland, Amsterdam, 1974
- [20] S. Lopez, A. Ortiz, *Semicond. Sci. Technol.* **9**, 2130 (1994)